Biofidelity and Limitations of Instrumented Mouthguard Systems for Assessment of Rigid Body Head Kinematics

Mitchell Z. Abrams, Jay Venkatraman, Donald Sherman, Maria Ortiz-Paparoni, Jefferson R. Bercaw, Robert E. MacDonald, Jason Kait, Elizabeth Dimbath, Derek Pang, Alexandra Gray, Jason F. Luck, Cynthia A. Bir, Cameron R. Bass

Abstract Instrumented mouthguard systems are used to study rigid body head kinematics *in vivo* in a variety of athletic environments. Previous work has assessed these systems when rigidly attached to anthropomorphic test device (ATD) heads and found good fidelity compared with reference sensors. Here, we examine the fidelity of two instrumented boil-and-bite mouthguards (iMGs) in helmeted, human cadaver impact tests at three velocities and three impact locations. The Prevent Biometrics iMG correlates with reference linear acceleration up to approximately 60 g, underestimating impacts at higher magnitudes. The Prevent iMG correlates well with angular velocity, while underestimating angular acceleration past approximately 3,000 rad/s^2. The DTS iMG consistently overestimates angular acceleration and velocity, and transformed linear kinematics are not well-correlated to reference kinematics at the head centre of gravity (HCG) for these impact conditions. Future work should examine the influence of the mandible and subject-specific mouthguard fit on fidelity of impact kinematics. This study highlights the need for cadaver validation studies of wearable head impact instrumentation systems, particularly when considering realistic (non-idealised) sensor-skull coupling and accounting for interactions with the mandible.

Keywords Cadaver, head impact exposure, mouthguard, wearable sensor, validation testing.

I. INTRODUCTION

Concussion is an important public health issue, with sports-related TBI affecting between 1.6 and 3.8 million individuals per year in the USA [1]. These estimates may be conservative, since 30–50% of concussions may go unreported [2-4]. Sports-related TBI accounts for up to one-third of all TBI cases presenting to the hospital [5]. Specifically, American football is associated with one of the highest rates of concussion, affecting 15.4% of youth football players [6-7].

During a head impact, a combination of linear and angular acceleration can produce brain injuries. Initial efforts to use head kinematics to predict the risk of injury focused on linear acceleration, resulting in the Wayne State Tolerance Curve and eventually the Head Injury Criterion (HIC) [8-10]. The Brain Injury Criterion (BrIC) was later developed to account for angular velocity, and so-called 'critical values' depend on direction of rotation [11]. Use of high-fidelity, non-invasive instrumentation *in vivo* is necessary for elucidating the biomechanics that cause TBI, and for assessing injury risk during real-world head impact events.

Systems such as the Head Impact Telemetry (HIT) System and skin-mounted systems such as the xPatch have been shown to have high error when compared with reference sensors in both linear [12-13] and angular kinematics [12-14]. Other studies have used sensors embedded in a mouthguard. Instrumented mouthguards (iMGs) are moulded to the dentition directly and record more accurate results than skin sensors [13]. In general, iMGs have performed well in laboratory testing with ATDs [15-19] and cadavers [19].

The iMG developed by Prevent Biometrics (Prevent Biometrics, Edina, MN, USA) provides 6 degrees of freedom (6DOF) linear and rotational kinematic data. The Prevent iMG has been previously validated with impact testing to 100 g using a modified Hybrid III ATD head, where it demonstrated mean relative errors of 8.3%, 4.7% and 3.4% for peak angular acceleration, angular velocity and linear acceleration, respectively [17]. Prevent has two versions of this iMG, a custom-fit model and a boil-and-bite model. While the custom iMG has better fit and accuracy, the boil-and-bite is easier to mould to an individual's dentition, is more scalable, and is the version used in the current study [17]. Other ATD studies also report a good correlation of mouthguard-to-reference in linear acceleration and angular velocity for the Prevent iMG when compared with the data obtained from reference sensors [15-16].

M. Z. Abrams (e-mail: mitchell.abrams@duke.edu; tel: +1 919-660-8274) is a PhD Candidate, M. Ortiz-Paparoni is a Postdoctoral Associate, J. Kait is a Research & Development Engineer, J. R. Bercaw and E. Dimbath are PhD students, D. Pang is a Research Associate, A. Gray is an Undergraduate Researcher, J. F. Luck is a Research Scientist, and C. R. Bass is an Associate Research Professor of Biomedical Engineering, all at Duke University in Durham, NC, USA. J. Venkatraman is a PhD Candidate, D. Sherman is on the research staff, R. E. MacDonald is a Research Assistant, and C. A. Bir is Chair and Professor of Biomedical Engineering at Wayne State University, Detroit, MI, USA.

The iMG developed by Diversified Technical Systems (DTS) (Diversified Technical Systems, Seal Beach, CA, USA) was part of an effort with the National Football League (NFL) to measure head kinematics. The DTS iMG has linear and angular accelerometers capable of measuring data in 6DOF. It records linear and angular acceleration up to 400 g's and 15,000 rad/s^2, respectively [20]. The correlation for the peak linear acceleration, peak angular velocity and peak angular acceleration compared to the reference sensor in a modified HIII ATD head for impact tests was R^2= 0.99 for all three metrics [20].

To date, these mouthguards have been assessed in idealised laboratory impact conditions using ATDs and in individuals participating in real sporting events (football and boxing), but no study has compared and validated the efficacy of these mouthguards in human cadavers that allow for realistic sensor-skull coupling while subjected to higher intensity impacts than observed in the prior volunteer studies [16][21-22]. In addition, these iMGs have only reported results up to 150 g's in ATDs [16-17][19-20][23-25]. Given that there have been reports of players experiencing peak linear acceleration over 200 g's in collegiate football [24] and 191 g's in boxing [25], it is imperative to compare and assess the accuracy of these iMGs in impacts across a range of impact severities. This study compares the response of two iMGs with rigidly mounted reference sensors in human cadaver heads.

II. METHODS

Specimen Preparation

Two unembalmed human cadaver heads were disarticulated at the atlanto-occipital joint (OC-C1). Soft tissue around the foramen magnum was removed to accommodate a (6DOF) reference sensor (6DX Pro, Diversified Technical Systems, Seal Beach, CA). An aluminium mounting plate was rigidly fixed to each head on the occipital bone adjacent to the foramen magnum to attach the 6DOF reference sensor. Impressions of the upper dentition were made for each cadaver and used to mould the iMGs following the manufacturers' instructions. The Prevent iMG and DTS iMG were submerged in boiling water, then fit with manual pressure to either the upper dentition of the cadaver or the dental mould. Specimens were scanned using computed tomography (CT) at 100 µm x 100 µm x 100 µm resolution (Nikon XTH 225 ST, Nikon Metrology Inc., Brighton, MI, USA) while instrumented with the 6DOF mounting plate and each mouthguard.

Coordinate frame transformation matrices were calculated and used to transform reference and DTS mouthguard kinematics to each head centre of gravity (HCG), and to express kinematic signals within a head coordinate system (HCS). The specimen HCG was computed from CT scan slices using a custom algorithm that segments cortical bone from soft tissue (MATLAB R2022b, Natick, Massachusetts). Each volume element was identified as either cortical bone or tissue and was assigned densities of 1.92 g/cm^3 or 1 g/cm^3, respectively [26]. The HCG was then computed by summing the mass and location of each volume element and dividing it by the total mass of the specimen. Anatomical landmarks were identified within the image to define the Frankfort plane as in [27]. HCS was defined, where the X and Y axes are within the Frankfort plane, and where X points anteriorly, Y points to the cadaver's left, and Z points superiorly. Additionally, locations and orientations of the reference sensor and DTS iMG were identified within the image by constructing a 3-dimensional model from CT slices and locating the (x,y,z) coordinates of the sensors. Transformation matrices $Q_{i\to s}$ (transformation from the CT image coordinate frame to the sensor recording frame) and $Q_{s\to HCS}$ (transformation from the sensor recording frame to the HCS) were determined from these (x,y,z) coordinates identified from the CT data:

$$Q_{i\to s} = \begin{bmatrix} \hat{\boldsymbol{x}}_{\boldsymbol{s}} \\ \hat{\boldsymbol{y}}_{\boldsymbol{s}} \\ \hat{\boldsymbol{z}}_{\boldsymbol{s}} \end{bmatrix} = \begin{bmatrix} x_x & x_y & x_z \\ y_x & y_y & y_z \\ z_x & z_y & z_z \end{bmatrix} \tag{1}$$

Angular acceleration at the HCS was determined with:

$$\vec{\alpha}_{HCS} = Q_{s\to HCS} * \vec{\alpha}_s, \tag{2}$$

Where $\vec{\alpha}_{HCS}$ is angular acceleration at the HCS, $Q_{s\to HCS}$ is the transformation matrix from the sensor frame to the HCS, and $\vec{\alpha}_s$ is angular acceleration in the sensor frame. Angular velocity was determined at the HCS by multiplying with $Q_{s\to HCS}$ as with angular acceleration in Eq 2. Linear acceleration at the HCG was found with:

$$\vec{a}_{CG} = \vec{a}_s + (\,\vec{\alpha}_s \, x \, \vec{r}\,) + \,\vec{\omega}_s \, x \,(\,\vec{\omega}_s \, x \, \vec{r}\,), \tag{3}$$

where $\vec{a}_s$, $\vec{\alpha}_s$, and $\vec{\omega}_s$ are the linear acceleration, angular acceleration, and angular velocity recorded in the sensor recording frame at the sensor location. The position vector $\vec{r}$ points from the sensor to the specimen centre of mass and is expressed in the sensor recording coordinate frame. $\vec{a}_{CG}$ is then multiplied with $Q_{S\rightarrow HCS}$ as in Eq 2 to determine acceleration at the HCG, in the HCS.

This estimation method is subject-specific, in contrast to the internal algorithm used by the Prevent iMG to estimate the HCG and orient to the HCS. No transformations were implemented for the Prevent iMG because it uses an internal algorithm to transform kinematic signals to an estimated head centre of mass and orient to the HCS. As a result, the estimated HCG for the reference transformations may not be identical to the location at which the Prevent iMG transforms the data.

Data Processing: Reference Sensors

Reference sensor data were collected at 100,000 samples/second with a 20 kHz hardware anti-aliasing filter. A total of 1.5 s of data were recorded for each impact, including 0.5 s of pre-trigger data. Linear acceleration and angular rate data were demeaned by subtracting the mean value of each channel during the first 5 ms from the entire signal for each trial. An 8-pole, 1,650 Hz phaseless, low-pass, Butterworth filter was used to remove high frequency noise. Angular acceleration was calculated from angular velocity using an 11-point central difference approximation. Angular velocity and angular acceleration were filtered with an 8-pole, 300 Hz phaseless, low-pass, Butterworth filter prior to translating linear kinematics to the HCG. Peak linear acceleration (PLA) was calculated as the maximum value of the resultant at the HCG. Peak angular velocity (PAV) and peak angular acceleration (PAA) were calculated as the maximum value of the resultant within 10 ms of PLA at the HCG from 300 Hz filtered data. HIC, HIC duration, and BrIC were calculated at the HCG.

Data Processing: Prevent iMG

The Prevent iMG contained a triaxial accelerometer (+/- 200 g full-scale range) and a triaxial gyroscope (+/- 35 rad/s full-scale range) sampling at 3,200 Hz [23]. For each impact, the Prevent iMG recorded 10 ms pre-trigger data and 40 ms post-trigger data. Mouthguard fit was assessed with a proximity sensor, and events were triggered using a 5 g threshold. The Prevent iMG communicates with the Prevent Web Portal to perform a variety of data analysis tasks prior to reporting impact attributes to the end user. The Prevent Web Portal reported: a) PLA, PAV and PAA values for each impact at the estimated HCG; and b) kinematic signals for each impact at the estimated HCG and oriented to the estimated HCS.

Following an impact event, the Prevent iMG transferred data to a mobile app via Bluetooth, then uploaded data to its server for processing. Prevent filtered the kinematic signals from all events with a 4-pole, phaseless, low-pass, Butterworth filter with a cut-off frequency of 200 Hz, and transformed them to an estimated HCG [23]. The Prevent Web Portal reported PLA, PAV and PAA from these 200 Hz filtered data. Further, an in-house Prevent algorithm classified each impact as low noise (class 0), moderate noise (class 1), or high noise (class 2), and assigned them cut-off frequencies of 200 Hz, 100 Hz, or 50 Hz, respectively [23][28]. Kinematic traces (linear acceleration vs. time, angular velocity vs. time, and angular acceleration vs. time) were filtered by Prevent at these additional cut-off frequencies with a 4-pole, phaseless, lowpass, Butterworth filter. We downloaded these filtered kinematic traces from the Prevent Web Portal and used the filtered signals to calculate HIC, HIC duration and BrIC as reported in this study.

Prevent's noise classification filtering scheme did not affect PLA, PAV and PAA values as reported in this study, as all peaks were provided by Prevent from kinematic signals that were filtered to 200 Hz. However, the noise classification filtering scheme *did* affect HIC, HIC duration and BrIC values, as these values were computed directly from the variably-filtered kinematic signals as outputted from the system.

Data Processing: DTS iMG

The DTS iMG contains a triaxial linear accelerometer (+/- 400 g full-scale range) and a triaxial angular accelerometer (+/- 15,000 rad/s^2) sampling at 5,500 Hz, with a 10 g trigger threshold. For each impact, DTS iMG recorded 10.55 ms pre-trigger and 100 ms post-trigger data. All data processing with DTS iMG data were performed by the research team. Angular and linear acceleration were demeaned by subtracting the mean value of each channel during the first 5 ms from the entire signal for each trial. Angular velocity was calculated from angular acceleration with a cumulative trapezoidal approximation. Data were filtered with an 8-pole, 1,650 Hz phaseless, low-pass, Butterworth filter and transformed to the HCG as described above for the reference. PLA, PAV and PAA were calculated as the maximum resultant at the HCG. HIC, HIC duration and BrIC were calculated at the HCG.

Experimental Testing

A linear impactor (Cadex, QC, Canada) with a steel spherical impactor head (11.43 cm radius) was used to impact the helmeted specimens. A previously untested, properly sized Riddell SpeedFlex helmet was used for all impacts. Three impact locations were marked on the helmet: front, lateral and rear. The helmet was impacted from the right side for the lateral impacts through approximately the HCG. Side impacts were located as defined in Fig. 1, 135 mm superior to the base of the helmet when placed on a horizontal flat surface, and 160 mm anterior to a plane tangent to the rear of the helmet and normal to the horizontal flat surface. Front- and rear-impact locations were on the midline of the helmet and located 39° and 45°, respectively, in elevation from the side-impact location in a transverse plane defined in Fig. 1. Each specimen was impacted three times at three velocities – low (4.2 m/s), medium (6.4 m/s) and high (7.8 m/s) – at all three impact locations for each mouthguard for a total of 27 impacts per mouthguard condition and 54 impacts total per specimen. Specimens were instrumented with the Prevent iMG, and impacted at the front, rear, and side locations, at increasing impact velocities. Specimens were then instrumented with the DTS iMG, and impacted at the side, rear, and front at increasing impact velocities. After the mouthguard was placed on the specimen's dentition and the helmet was fitted onto the specimen, the chin strap was pulled tight to ensure that the lower dentition was in contact with the mouthguard, until the mandible was determined to be immobile. The straps were tightened to ensure the jaw was pulled up to engage the mouthguard, rather than towards the posterior. The specimens were suspended inside a mesh bag, allowing free movement following impact. Due to movement of the specimen and collision with the test enclosure, the iMGs reported multiple impacts for each test. Any subsequent impacts after the initial event were not considered in the analysis. The reference block was checked at the beginning and end of the test series to ensure it remained rigidly fixed to the skull. Both the chinstrap and the jaw were observed to be unmoved between tests, and the chinstrap was tightened as needed.

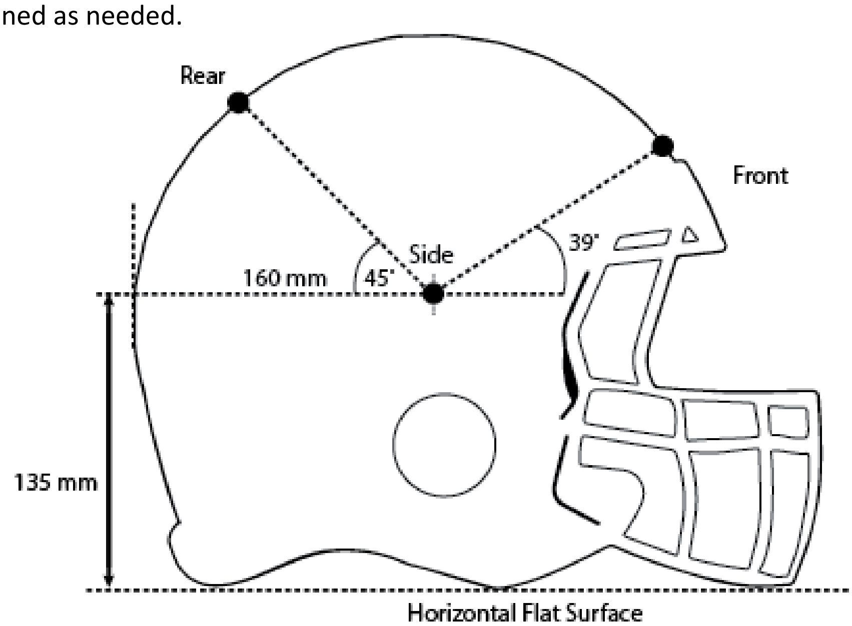

Fig. 1. Side impacts were 135 mm superior to a horizontal plane aligned with the base of the helmet, and 160 mm anterior to a plane tangent to the rear of the helmet and normal to the horizontal flat surface. Front and rear impacts were along the midline, 39° and 45° in elevation from the side impact location in a transverse plane, respectively.

III. RESULTS

Prevent iMG

The Prevent iMG correlated with reference results for PLA up to 60 g (deviating from reference by less than 5%), underestimating PLA reference sensor values at higher magnitudes (deviating from reference by 50% at 200 g) (Fig. 2). For low-velocity, front impacts (Prevent PLA = 54 ± 6 g; Reference PLA = 59 ± 8 g), rear impacts (Prevent PLA = 60 ± 1 g; Reference PLA = 71 ± 12 g) and side impacts (Prevent PLA = 46 ± 3g; Reference PLA = 45 ± 11g), the Prevent iMG reported PLA values similar to the reference. At medium- and high-velocity impact conditions, Prevent iMG underestimated the reference, as seen in Fig. 2 and Appendix A, Table AI (cf. medium-velocity front impacts: Prevent PLA = 84 ± 17 g; Reference PLA = 118 ± 10 g; high-velocity side impacts: Prevent PLA = 88 ± 2 g; Reference PLA = 200 ± 51 g). Overall, the Prevent iMG PLA approximates a quadratic fit to the reference data (R^2 = 0.729).

PAV values reported by the Prevent iMG software were similar to reference values across impact cases (Prevent iMG PAV = 0.872*Reference, R^2 = 0.908; cf. low-velocity side impacts: Prevent PAV = 13 ± 2 rad/s; Reference PAV = 12 ± 2 rad/s; see Appendix A, Table AI). For high-velocity side impacts (Prevent PAV = 25 ± 2 rad/s; Reference PAV = 30 ± 4 rad/s) and front impacts (Prevent PAV = 13 ± 3 rad/s; Reference PAV = 17 ± 2 rad/s), Prevent iMG underestimates the reference. The linear fit to reference PAV deviated by 13% across the range.

PAA values were similar for low-velocity side impacts (Prevent PAA = 2,345 ± 430 rad/s^2; Reference PAA = 2,361 ± 339 rad/s^2), medium-velocity rear impacts (Prevent PAA = 1,629 ± 439 rad/s^2; Reference PAA = 1,116 ± 501 rad/s^2) and high-velocity rear impacts (Prevent PAA = 2,345 ± 430 rad/s^2; Reference PAA = 2,361 ± 339 rad/s^2) when compared to the reference. For all other cases, Prevent iMG underestimated the reference (cf. high-velocity front impacts, Prevent PAA = 1780 ± 521 rad/s^2; Reference PAA = 5,960 ± 1,285 rad/s^2, see Appendix A, Table AI) and was not well correlated with reference values (Prevent PAA = 0.396*Reference; R^2 = -0.325), deviating by 60% of reference across the range.

BrIC values from the Prevent iMG correlated well with the reference for low-velocity impacts (cf. low-velocity side impacts: Prevent BrIC = 0.22 ± 0.04; Reference BrIC = 0.24 ± 0.08), medium-velocity front impacts (Prevent BrIC = 0.31 ± 0.1; Reference BrIC = 0.19 ± 0.06), and high-velocity front impacts (Prevent BrIC = 0.3 ± 0.08; Reference BrIC = 0.31 ± 0.03). In general, BrIC values from the Prevent iMG agreed with the reference for front impacts. For medium- and high-velocity side impacts, Prevent BrIC values are underestimated compared to the reference, while for medium- and high-velocity rear impacts Prevent overestimated BrIC (Appendix A, Table AI).

The Prevent iMG software underestimated HIC for all conditions except low-velocity side impacts (Prevent HIC = 64 ± 6; Reference HIC = 57 ± 35). For some conditions, the reported HIC value was less than half the reference value (cf. medium-velocity front impacts: Prevent HIC = 175 ± 122; Reference HIC = 440 ± 103). HIC duration was similar between the Prevent iMG and reference for low- and medium-velocity front impacts, low- and medium-velocity side impacts, and medium-velocity rear impacts. BrIC, HIC and HIC duration were calculated from kinematic traces, which were filtered at either 200 Hz, 100 Hz, or 50 Hz depending on the noise classification level that Prevent determined for each impact. Figure 3 shows linear and angular kinematics for a representative high-velocity frontal impact. Mean impact metrics are provided in Appendix A, Table AI for each impact condition.

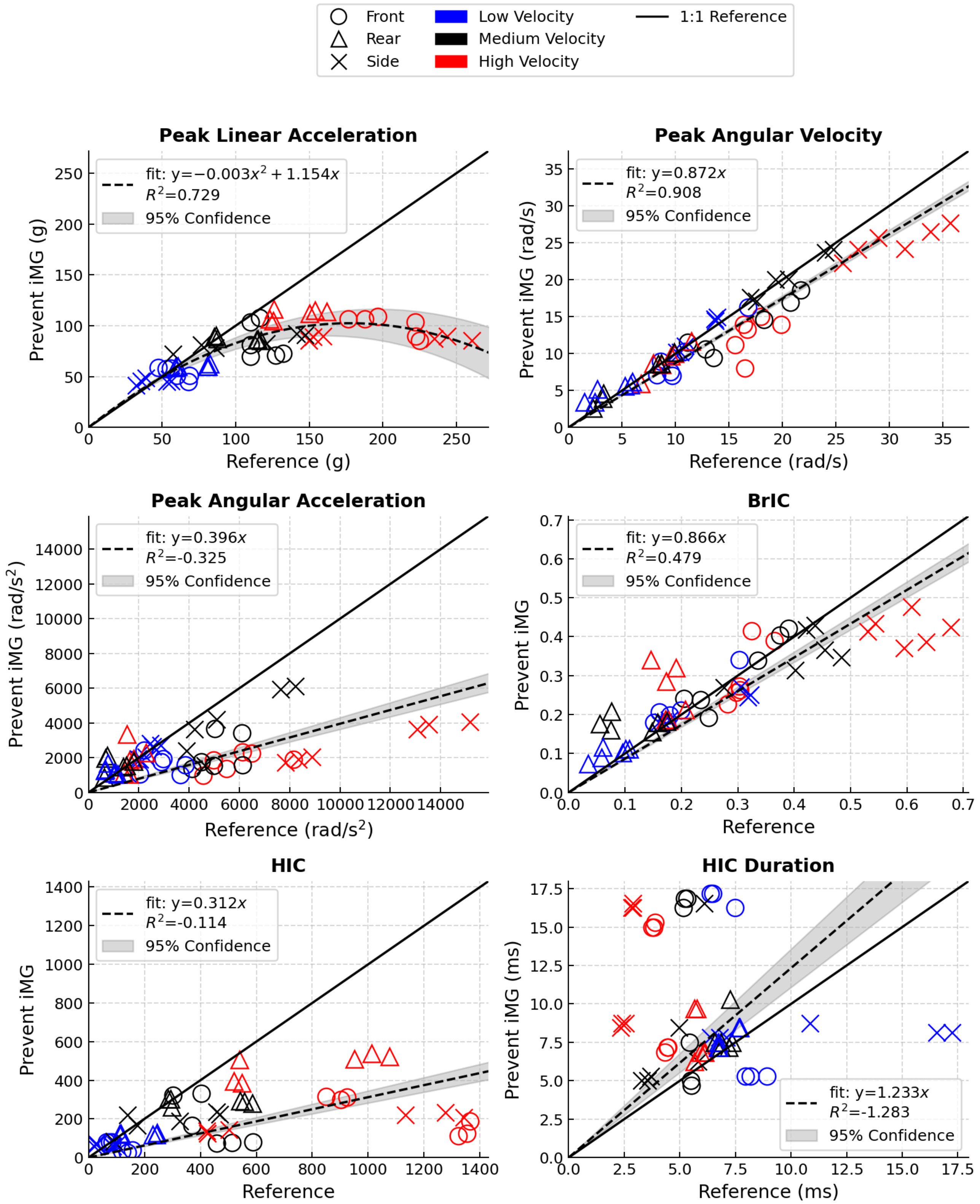

Fig. 2. Prevent iMG compared to reference for peak linear acceleration (top left), peak angular velocity (top right), peak angular acceleration (middle left), BrIC (middle right), HIC (bottom left), and HIC duration (bottom right). Peak linear acceleration, peak angular velocity, and peak angular acceleration were all calculated from kinematic signals filtered at 200 Hz. BrIC, HIC and HIC duration were calculated from kinematic signals filtered at either 200 Hz, 100 Hz, or 50 Hz.

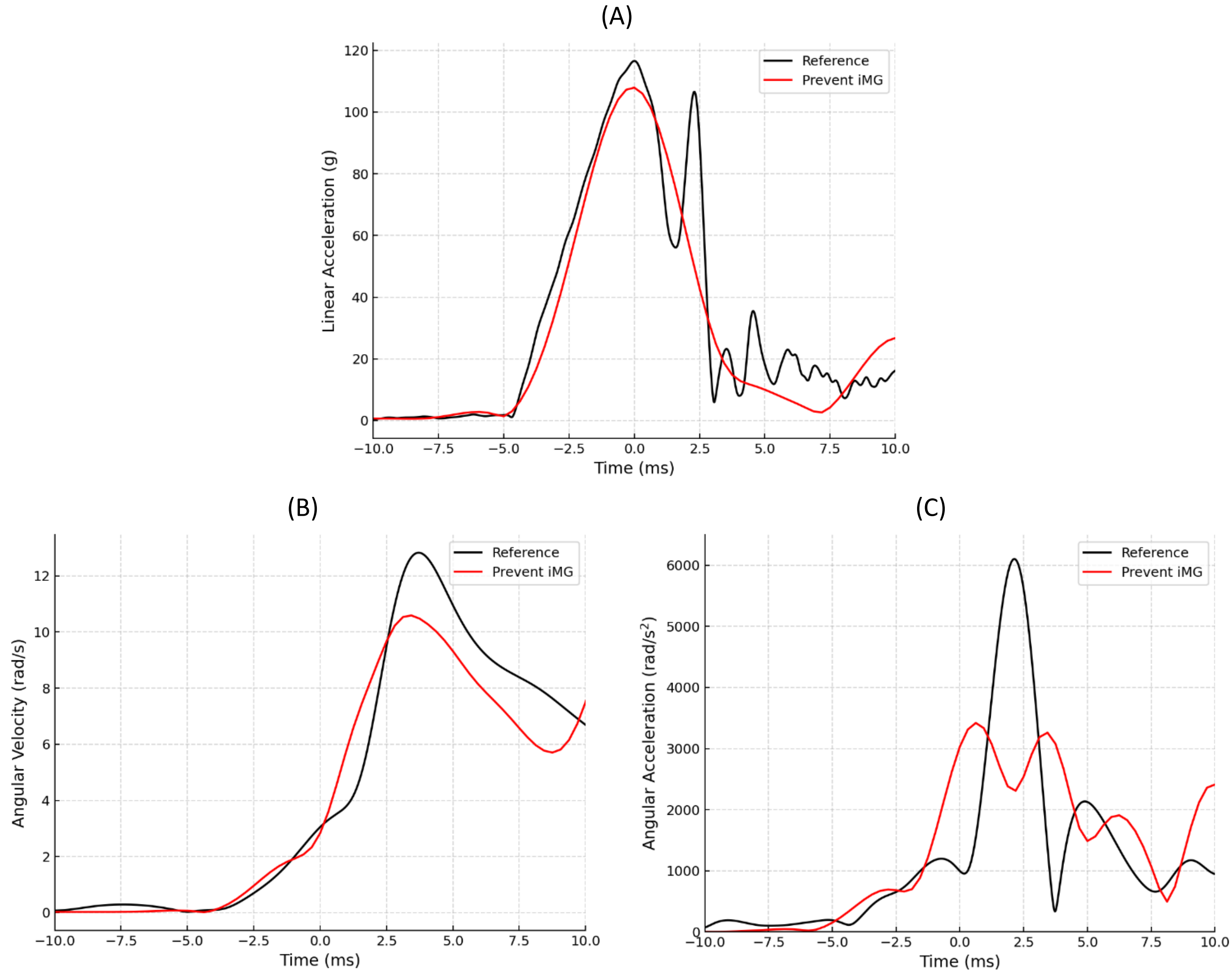

Fig. 3. Linear acceleration (A), angular velocity (B) and angular acceleration (C) for reference and Prevent iMG during a high-velocity rear impact. For this impact, Prevent PLA = 108 g, PAV = 11 rad/s, PAA = 3,420 rad/s^2, HIC = 331, duration = 4.7 ms, BrIC = 0.24. Reference PLA = 117 g, PAV = 13 rad/s, PAA = 6,103 rad/s^2, HIC = 403, duration = 5.5 ms, BrIC = 0.23. Prevent iMG labelled this impact as low noise (class 0), and filtered with a 200 Hz, low pass filter. Reference linear kinematics were filtered at 1,650 Hz, and angular kinematics were filtered at 300 Hz.

DTS iMG

The DTS iMG was similar to the reference sensor for rear impacts in PLA at low (DTS PLA = 79 ± 30 g; Reference PLA = 67 ± 11 g), medium (DTS PLA = 113 ± 38 g; Reference PLA = 101 ± 22 g) and high velocities (DTS PLA = 165 ± 58 g; Reference PLA = 146 ± 25 g) (Fig. 5). Further, the DTS iMG PLA was similar to the reference for side impacts at low (DTS PLA = 58 ± 7 g; Reference PLA = 49 ± 10 g) and medium velocities (DTS PLA = 137 ± 20 g; Reference PLA = 101 ± 42 g). For all other impacts, the DTS iMG overestimated PLA when compared to the reference values (cf. low-velocity front impacts: DTS PLA = 219 ± 48 g; Reference PLA = 63 ± 21 g; see also Fig. 5 and Appendix A, Table AII).

The DTS iMG overestimated PAA compared to the reference under all conditions, reporting values twice that of the reference (cf. medium-velocity side impacts: DTS PAA = 9,649 ± 2,456 rad/s^2; Reference PAA = 6,449 ± 1,534 rad/s^2), with poor correlation (DTS PAA = 2.054 * Reference, R^2 = 0.114, Fig. 5). Angular velocity was calculated from angular acceleration filtered at 300 Hz. The DTS PAV overestimated reference values (filtered at 300 Hz) for all impact conditions (cf. medium-velocity side impacts: DTS PAV = 34 ± 2 rad/s; Reference PAV = 23 ± 1 rad/s; see Fig. 5 and Appendix A, Table AII). DTS PAV was poorly correlated with the reference (DTS PAV = 1.919 * Reference, R^2 = -0.483). The DTS iMG calculated BrIC values that were similar to the reference for low-velocity side impacts only (DTS BrIC = 0.33 ± 0.06; Reference BrIC = 0.24 ± 0.06). For all other test cases, the DTS iMG overestimated BrIC values compared to the reference (DTS BrIC = 1.947 * Reference, R^2 = -0.636).

HIC values from the DTS iMG were similar to the reference for rear impacts at low (DTS HIC = 276 ± 301; Reference HIC = 166 ± 71), medium (DTS HIC = 447 ± 219; Reference HIC = 440 ± 214) and high velocities (DTS HIC = 835 ± 437; Reference HIC = 782 ± 327), as well as for side impacts at low velocity (DTS HIC = 110 ± 15; Reference HIC = 64 ± 41). For other conditions, the DTS iMG overestimated HIC values, compared to the reference, by a factor of two to five (cf. medium-velocity front impacts: DTS HIC = 1,249 ± 818; Reference HIC = 457 ± 206). The HIC durations calculated from the DTS iMG data were similar to the reference values for rear impacts (cf. rear impacts at low velocity: DTS HIC duration = 7.2 ± 1.1 ms; Reference HIC duration = 7.3 ± 0.3 ms), side impacts at low (DTS HIC duration = 7.5 ± 0.8 ms; Reference HIC duration = 5.9 ± 1.3 ms) and medium velocities (DTS HIC duration = 4.2 ± 1.2 ms; Reference HIC duration = 4.5 ± 1.1 ms), and front impacts at medium velocity (DTS HIC duration = 5.7 ± 1.3 ms; Reference HIC duration = 5.0 ± 1.1 ms) (Appendix A, Table AII). Representative linear acceleration, angular velocity and angular acceleration traces are shown in Fig. 4 for a front, high-velocity impact.

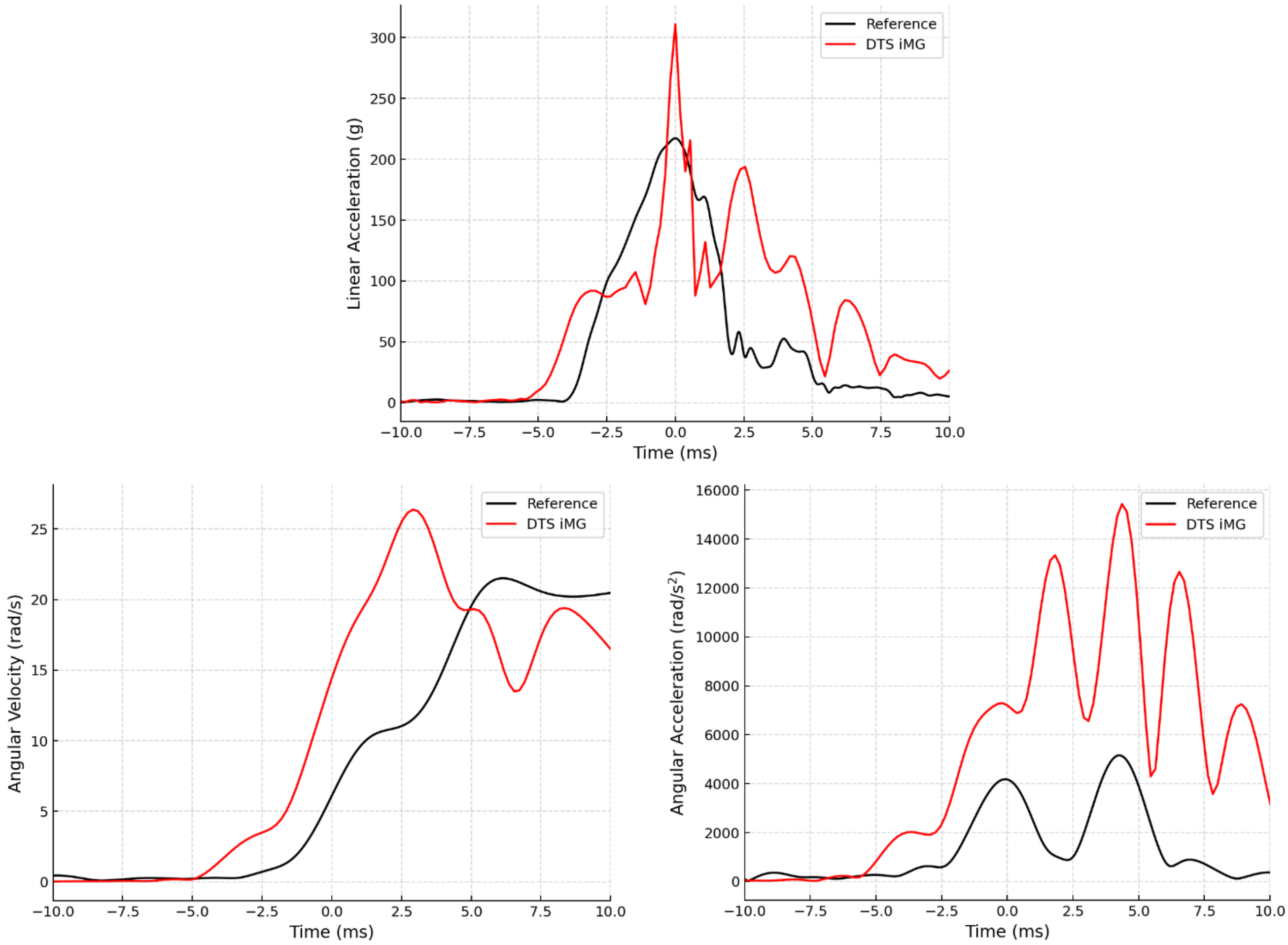

Fig. 4. Linear acceleration (A), angular velocity (B) and angular acceleration (C) for reference and DTS iMG during a high velocity (7.88 m/s) front impact. For this impact, DTS PLA = 311 g, PAV = 27 rad/s, PAA = 15,434 rad/s^2, HIC = 1,647, duration = 8.5 ms, BrIC = 0.55. Reference PLA = 217 g, PAV = 22 rad/s, PAA = 5,155 rad/s^2, HIC = 1,495, duration = 4.2 ms, BrIC = 0.41. All linear kinematics were filtered at 1650 Hz, and angular kinematics were filtered at 300 Hz.

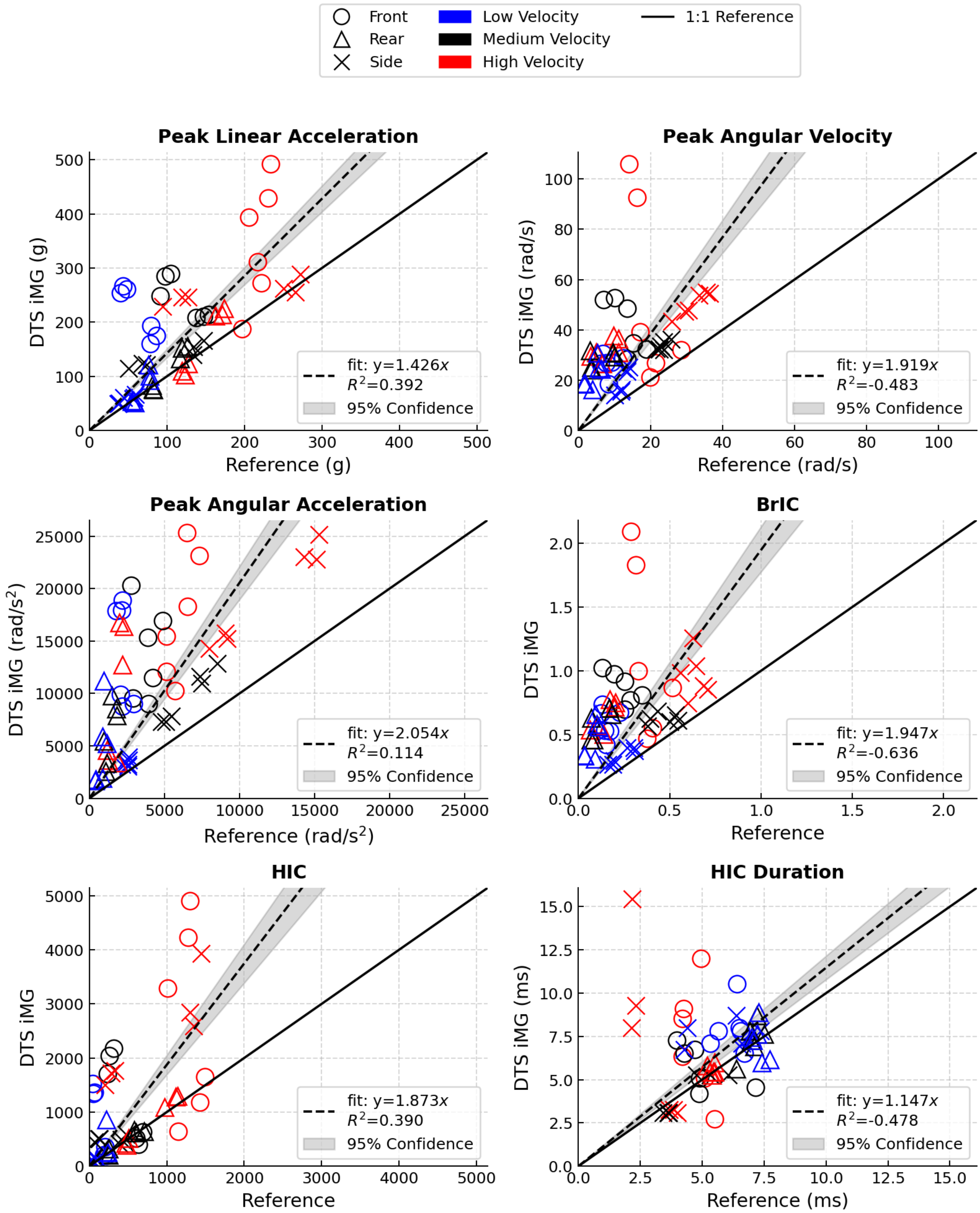

Fig. 5. DTS iMG compared to reference for peak linear acceleration (top left), peak angular velocity (top right), peak angular acceleration (middle left), BrIC (middle right), HIC (bottom left) and HIC duration (bottom right). All linear kinematics were filtered at 1650 Hz, and angular kinematics were filtered at 300 Hz.

IV. Discussion

In peak linear acceleration, the Prevent iMG showed agreement with the reference sensor up to 60 g, where it began to diverge from the reference sensor for all three impact locations by more than 5% (Fig. 2). In angular velocity, the Prevent iMG underestimated PAV for high-velocity front and side impacts, but was similar to the reference PAV in low- and medium-velocity impacts. In PAA, the Prevent iMG was similar to the reference for low-velocity side and rear impacts, as well as for high-velocity rear impacts, but underestimated PAA when compared to higher reference PAAs. The Prevent iMG underestimated HIC for medium- and high-velocity impacts, and overestimated HIC duration across conditions. Prevent iMG correlated well with the reference for BrIC values at low and medium velocities, but not for high-velocity impacts.

The Prevent iMG has a noise classification filtering scheme, wherein each impact was classified as low noise (class 0), moderate noise (class 1), or high noise (class 2). The algorithm filters each noise class (low, moderate, or high noise) differently using cut-off frequencies of 200 Hz, 100 Hz, or 50 Hz, respectively [28]. We used these filtered kinematic signals to calculate HIC, HIC duration and BrIC as reported in this study, which may explain the tendency of the Prevent iMG to underestimate injury metrics and to overestimate impact duration compared to the reference sensor. However, all PLAs, PAVs and PAAs from the Prevent iMG were reported from kinematic signals that were filtered with a cut-off frequency of 200 Hz. Therefore, the performance of the Prevent system in estimating PLA, PAV and PAA is unaffected by the noise classification filtering scheme. Future work should use the raw data from the Prevent iMG for calculated injury metrics, rather than the provided filtered traces. The Prevent iMG uses a proximity sensor to determine whether the mouthguard is on the dentition or not. In consultation with Prevent, the threshold value for "on/off the teeth" was lowered to account for potential differences in enamel reflectivity between the cadaver dentition and live human subjects. For all but three impacts, the pre- and post-impact proximity readings were largely unchanged, likely indicating the mouthguard remained coupled during the impact events. The DTS iMG systematically overestimated PLA (Fig. 5) but was better correlated with the reference PLA for rear and side impacts as opposed to front. In both PAV and PAA, the DTS iMG overestimated the reference in all impacts. The DTS iMG did not correlate well with the reference for HIC or BrIC values, overestimating in both cases, and did not correlate well with HIC duration.

All data for the DTS iMG were rotated from the sensor coordinate system to the HCS and then translated to the HCG. Notably, the DTS iMG reported peak angular accelerations that were higher than the calculated reference angular acceleration (Fig. 5). The HCG translation relies heavily on angular kinematics to calculate linear acceleration at the target location (see Eq 3). Due to the overestimation in angular kinematics, the translation to the HCG results in much higher PLAs when compared to the reference. In contrast, when translating the reference sensor to the location of the DTS iMG sensor (and leaving the DTS iMG data untransformed), the linear kinematics of the DTS iMG agree with the reference sensor more closely. For comparison, Fig. 6 shows an example of a low-velocity front impact with both the iMG and reference sensor transformed to the HCG, and with the reference transformed to the DTS iMG sensor location. For this impact, the angular kinematics are orders of magnitude larger for the DTS iMG compared to the reference, fully dominating the translation to HCG. By transforming only the reference sensor kinematics to the DTS linear accelerometer, the error associated with the DTS iMG angular accelerometer can be removed, and the linear kinematics as reported by the DTS iMG can be compared to the reference. Without the influence of angular kinematics on the transform, DTS iMG PLA falls closer to the reference sensor (Fig. 7). While accuracy in linear kinematics is valuable, angular motion is suspected to play a large role in brain injury, and poor angular fidelity compromises the utility of the device in predicting brain injury.

A HIC greater than 1000 corresponds to a 50% risk for severe neurological injuries, and a HIC greater than approximately 670 corresponds to a 50% risk of skull fracture [29]. The Prevent iMG underestimates HIC consistently when the reference score is above 400. Relying solely on HIC to predict brain injury would result in underreported injury rates during field use. In contrast, the DTS iMG can overestimate HIC during medium- and high-velocity impacts. While more conservative estimates of HIC would minimise risk of missing injurious events on the field, an accurate metric is ideal to further understand underlying biomechanical behaviours.

Our findings contrast with previously published validation studies of both the Prevent iMG and the DTS iMG. Helmeted impact tests on ATDs instrumented with the Prevent iMG suggest a nearly one-to-one relationship between mouthguard kinematics and ATD reference values [16-18][23]. However, in [18], iMGs were clamped to ATD dentition, effectively forcing a rigid coupling. While this may be representative of a tightly clenched jaw condition, not all impacts can be assumed to occur under those conditions. In [17], a mobile mandible was constrained to prevent contact with the iMG under any condition, eliminating the influence of the mandible from the test. ATD impact tests under both helmeted and unhelmeted conditions, with constrained and free ATD mandibles, similarly showed a nearly one-to-one response of the Prevent iMG up to 150 g [16]. However, that study did not report the characteristics or processing of the reference system, limiting comparison to the results presented here. Similarly, validation studies of the DTS iMG have found nearly one-to-one accuracy during ATD testing in both helmeted and unhelmeted test scenarios [20][23]. In both [23] and [20], the mandible was clamped to the upper dentition, as in [18].

Previous work has shown that an unconstrained mandible can result in poor accuracy of mouthguard-reported kinematics when compared to a reference in both ATD and cadaver testing [19]. Here, the only constraint on the mandible is the tightened chinstrap of the helmet, which could allow for jaw movement and interaction with the mouthguard. At higher impact magnitudes, this could result in larger mouthguard-mandible interaction, which may explain the more aggressive filtering applied to these conditions compared to low-velocity impacts for the Prevent iMG. When performing ATD testing, the mandible constraint must be carefully considered, to ensure the interaction between the mandible and the mouthguard is properly represented [19]. While this study constrained the mandible with the helmet chinstrap, the movement of the mandible was not measured, and the interaction between mandible and mouthguard could not be directly measured. While the chinstrap was tensioned until the jaw was deemed immobile, tension was not quantified or standardised beyond this qualitative assessment. This may introduce some of the variability in mouthguard results, but is unlikely to be the root cause of the discrepancies between iMG and reference data across all test conditions. The chinstrap was readjusted as needed between tests to ensure the jaw remained immobile.

In the absence of active musculature, the mandible may move more than when the jaw is actively clenched, resulting in 'jaw slap,' and erroneously high linear and angular acceleration measures as in [19]. The untransformed DTS iMG data (Fig. 7) overestimated the reference linear acceleration, and may be due to this phenomenon. However, the Prevent iMG consistently underestimated both angular and linear acceleration. Higher frequency content introduced by the mandible striking the mouthguard may be filtered by the Prevent algorithm, yet should not result in consistently lower estimates of head acceleration. Future work should examine the raw data from the Prevent system to identify whether mandible motion affects the sensor recordings at higher impact levels.

While some aspects of the methodology used for this study align with the Consensus Head Acceleration Measurement Practices (CHAMP) statement on laboratory validation of wearable sensors, such as the use of cadaver specimens, multiple samples of each mouthguard and a range of test conditions representative of on-field conditions [30], the ability of each iMG to detect an impact event was not assessed. For each impact, multiple subsequent events were recorded by both the Prevent iMG and DTS iMG due to free movement of the specimen and collisions with the test enclosure. While future work could compare subsequent events to ensure the iMGs record true collisions, the ability to discriminate between true and false positive events may be better suited to on-field video verification studies. Additionally, the current analysis does not account for the reported direction of impact (a feature of the Prevent iMG). Future studies should assess the accuracy of impact direction reporting for this device.

This study only examined helmeted impacts with boil-and-bite mouthguards. While football represents a large proportion of observed concussions, instrumented mouthguards are used in unhelmeted sports, such as martial arts and rugby league. Future studies should examine the performance of instrumented mouthguards during unhelmeted impact conditions. Custom fit mouthguards produced for subject-specific dentition may provide a tighter fit and better coupling, and should be examined in future work. No impacts were tested below 30 g. While both iMGs triggered for some secondary impacts, these were not matched to sub-30 g secondary events recorded by the reference sensor. Thus, we were unable to assess the performance of the iMGs in low-level impact conditions. The reference sensor (DTS 6DX Pro, 2000g full scale range) has a linearity of <1% full scale, corresponding to an overall accuracy of ±20 g, and ±3.14 rad/s. At the "worst-case" deviation from linear output, reference sensor error is insufficient to account for the difference between the reference linear acceleration for either the Prevent or DTS iMG. The angular velocity error similarly is insufficient to account for the differences between the reference and DTS iMG.

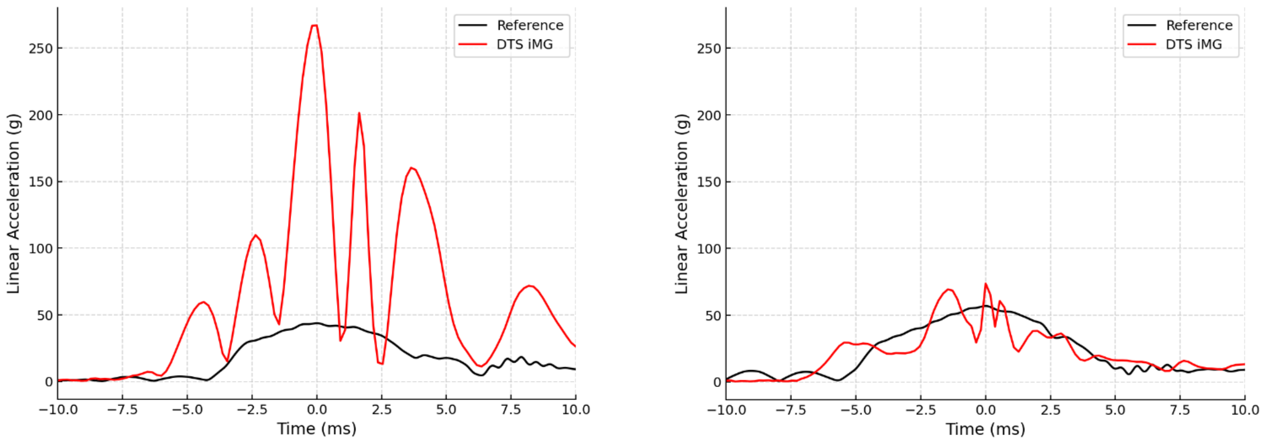

Fig. 6. DTS iMG and reference linear acceleration transformed to the head centre of gravity (left), and reference linear acceleration transformed to DTS sensor location (right). Linear kinematics are similar when angular kinematics do not affect the DTS transformation.

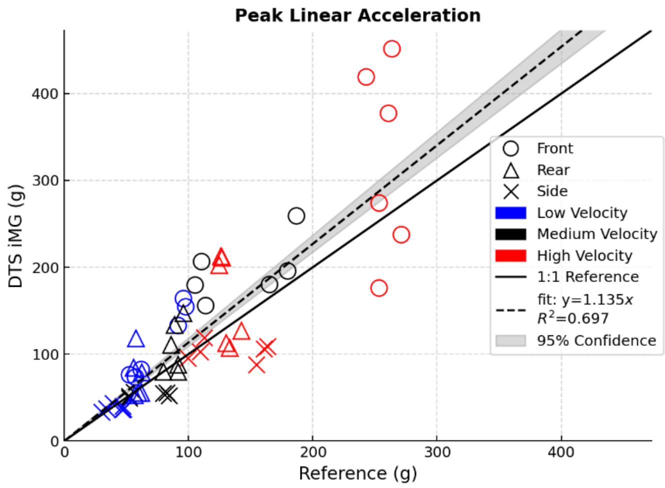

Fig. 7. Peak linear acceleration, DTS iMG vs. Reference, reference transformed to DTS sensor origin.

V. CONCLUSIONS

This study found that the Prevent iMG and the DTS iMG do not correlate with reference sensors across the range of tests performed. While the Prevent iMG correlates well with reference linear acceleration below 60 g, it underestimated linear acceleration at higher velocity impact conditions. Prevent correlates well with angular velocity and BrIC for low- and medium-velocity impacts. However, Prevent iMG consistently underestimates HIC and overestimates HIC duration. The internal filtering algorithm used by the Prevent iMG systematically reduces impact peaks relative to the rigid body head kinematic traces assessed using the reference sensor, affecting injury metric calculations. The DTS iMG systematically overestimates angular acceleration by more than 100%, complicating efforts to translate impact kinematics to the head centre of gravity. The qualitative difference between the cadaveric impact testing performed and previous assessments using ATDs emphasises the limitations of metallic headforms for validating wearable sensors for head impact monitoring. The findings here highlight the need for cadaver impact testing, especially for larger amplitude impact exposures, rather than rigidly fixing wearable devices to ATD headforms for idealised boundary conditions. Future work should assess surrogates applicable to validating human wearables *in vivo*. Such surrogates should have capabilities to assess limitations of mandible fit and should include appropriate jaw constraints to simulate realistic lower mandible secondary impacts on the instrumentation ('jaw slap').

VI. ACKNOWLEDGEMENTS

The authors gratefully acknowledge support from the Duke University Pratt School of Engineering, and the Wayne State University College of Engineering Department of Biomedical Engineering. The authors also wish to acknowledge the assistance of Kyvory Henderson at DTS and Adam Bartsch at Prevent for their assistance in configuring the mouthguards and interpreting their outputs.

VII. References

[1] Langlois, J. A., Rutland-Brown, W., Wald, M. M. (2006) The epidemiology and impact of traumatic brain injury: a brief overview. *The Journal of head trauma rehabilitation*, **21**(5): pp.375–378.

[2] McCrea, M., Hammeke, T., Olsen, G., Leo, P., Guskiewicz, K. (2004) Unreported concussion in high school football players: implications for prevention. *Clinical Journal of Sports Medicine*, **14**(1): pp.13–7.

[3] Williamson, I. J. S. and Goodman, D. (2006) Converging evidence for the under-reporting of concussions in youth ice hockey. *British Journal of Sports Medicine*, **40**(2): pp.128–32; discussion 128–32.

[4] Meehan, W. P., Mannix, R. C., O'Brien M. J., Collins, M. W. (2013) The prevalence of undiagnosed concussions in athletes. *Clinical Journal of Sports Medicine*, **23**(5): pp.339–42.

[5] Theadom, A., Mahon, S., *et al*. (2020) Incidence of Sports-Related Traumatic Brain Injury of All Severities: A Systematic Review. *Neuroepidemiology*, **54**(2): pp.192–199.

[6] Tsushima, W. T., Siu, A. M., Ahn, H. J., Chang, B. L., Murata, N. M. (2019) Incidence and Risk of Concussions in Youth Athletes: Comparisons of Age, Sex, Concussion History, Sport, and Football Position. *Archives of Clinical Neuropsychology*, **34**(1): pp.60–69.

[7] O'Connor, K. L., Baker, M. M., *et al*. (2017) Epidemiology of Sport-Related Concussions in High School Athletes: National Athletic Treatment, Injury and Outcomes Network (NATION), 2011-2012 Through 2013-2014. *Journal of Athletic Training*, **52**(3): pp.175–185.

[8] Versace, J. (1971) A Review of the Severity Index.

[9] Gurdjian, E. S., Roberts, V. L., Thomas, L. M. (1966) Tolerance curves of acceleration and intracranial pressure and protective index in experimental head injury. *Journal of Trauma*, **6**(5): pp.600–604.

[10] Mertz, H. J., Prasad, P., Nusholtz, G. (1996) Head injury risk assessment for forehead impacts. *SAE Transactions*, pp.26–46.

[11] Takhounts, E. G., Craig, M. J., Moorhouse, K., McFadden, J., Hasija, V. (2013) Development of brain injury criteria (BrIC). *Stapp Car Crash Journal*, **57**: pp.243–66.

[12] Jadischke, R., Viano, D. C., Dau, N., King, A. I., McCarthy, J. (2013) On the accuracy of the Head Impact Telemetry (HIT) System used in football helmets. *Journal of Biomechanics*, **46**(13): pp.2310–2315.

[13] Wu, L. C., Nangia, V., *et al*. (2016) In vivo evaluation of wearable head impact sensors. *Annals of Biomedical Engineering*, **44**(4): pp.1234–1245.

[14] Tiernan, S., Byrne, G., O'Sullivan, D. M. (2019) Evaluation of skin-mounted sensor for head impact measurement. *Proceedings of the Institution of Mechanical Engineers, Part H: Journal of Engineering in Medicine*, **233**(7): pp.735–744.

[15] Hedin, D. S., Gibson, P. L., Bartsch, A. J., Samorezov, S. (2016) Development of a head impact monitoring "Intelligent Mouthguard". *Annual International Conference of the IEEE Engineering in Medicine and Biology Society*, Berlin, Germany, pp.2007–2009.

[16] Bartsch, A. J., McCrea, M. M., *et al*. (2019) Laboratory and On-field Data Collected by a Head Impact Monitoring Mouthguard. *Annual International Conference of the IEEE Engineering in Medicine and Biology Society*, Berlin, Germany, pp.2068–2072.

[17] Liu, Y., Domel, A. G., *et al*. (2020) Validation and Comparison of Instrumented Mouthguards for Measuring Head Kinematics and Assessing Brain Deformation in Football Impacts. *Annals of Biomedical Engineering*, **48**(11): pp.2580–2598.

[18] Kieffer, E. E., Begonia, M. T., Tyson, A. M., Rowson, S. (2020) A Two-Phased Approach to Quantifying Head Impact Sensor Accuracy: In-Laboratory and On-Field Assessments. *Annals of Biomedical Engineering*, **48**(11): pp.2613–2625.

[19] Kuo, C., Wu, L. C., *et al*. (2016) Effect of the mandible on mouthguard measurements of head kinematics. *Journal of Biomechanics*, **49**(9): pp.1845–1853.

[20] Gabler, L. F., Dau, N. Z., *et al*. (2021) Development of a low-power instrumented mouthpiece for directly measuring head acceleration in American football. *Annals of Biomedical Engineering*, **49**(10): pp.2760–2776.

[21] Bartsch, A., Samorezov, S., Benzel, E., Miele, V., Brett, D. (2014) Validation of an "Intelligent Mouthguard" Single Event Head Impact Dosimeter. *Stapp Car Crash Journal*, **58**: pp.1–27.

[22] Jansen, A. E., McGrath, M., *et al*. (2021) Characterizing Head Impact Exposure in Men and Women During Boxing and Mixed Martial Arts. *Orthopaedic Journal of Sports Medicine*, **9**(12): p. 23259671211059815.

[23] Jones, B., Tooby, J., *et al*. (2022) Ready for impact? A validity and feasibility study of instrumented mouthguards (iMGs). *British Journal of Sports Medicine*. **56:** pp.1171-1179.

[24] Broglio, S. P., Sosnoff, J. J., *et al*. (2009) Head impacts during high school football: a biomechanical assessment. *Journal of Athletic Training*, **44**(4): pp.342–349.
[25] Stojsih, S., Boitano, M., Wilhelm, M., Bir, C. (2010) A prospective study of punch biomechanics and cognitive function for amateur boxers. *British Journal of Sports Medicine*, **44**(10): pp.725–730.
[26] O'Flaherty, E. J. (1991) Physiologically based models for bone-seeking elements. III. Human skeletal and bone growth. *Toxicology and Applied Pharmacology*, **111**(2): pp.332–41.
[27] Daboul, A., Schwahn, C., *et al*. (2012) Reproducibility of Frankfort horizontal plane on 3D multi-planar reconstructed MR images. *PLoS One*, **7**(10): p.e48281.
[28] Tooby, J., Weaving, D., Al-Dawoud, M., Tierney, G. (2022) Quantification of Head Acceleration Events in Rugby League: An Instrumented Mouthguard and Video Analysis Pilot Study. *Sensors (Basel)*, **22**(2).
[29] Marjoux, D., Baumgartner, D., Deck, C., Willinger, R. (2008) Head injury prediction capability of the HIC, HIP, SIMon and ULP criteria. *Accident Analysis and Prevention*, **40**(3): pp.1135–1148.
[30] Gabler, L., Patton, D., *et al*. (2022) Consensus Head Acceleration Measurement Practices (CHAMP): Laboratory Validation of Wearable Head Kinematic Devices. *Annals of Biomedical Engineering*, **50**(11): pp.1356–1371.

VIII. APPENDIX

TABLE AI
PREVENT IMG AND REFERENCE IMPACT METRICS

	Front (n=6)		**Rear (n=6)**		**Side (n=6)**	
	Reference	iMG	Reference	iMG	Reference	iMG
Low Velocity						
PLA	59 ± 8 g	54 ± 6 g	71 ± 12 g	60 ± 1 g	45 ± 11 g	46 ± 3 g
PAV	11 ± 3 rad/s	10 ± 4 rad/s	4 ± 2 rad/s	5 ± 1 rad/s	12 ± 2 rad/s	13 ± 2 rad/s
PAA	2931 ± 728 rad/s/s	1626 ± 540 rad/s/s	884 ± 215 rad/s/s	1260 ± 227 rad/s/s	2361 ± 339 rad/s/s	2345 ± 430 rad/s/s
HIC	107 ± 37	57 ± 26	176 ± 69	122 ± 4	57 ± 35	64 ± 6
HIC Duration	7.6 ± 1.0 ms	11.1 ± 6.3 ms	7.2 ± 0.5 ms	7.9 ± 0.6 ms	10.8 ± 5.0 ms	8.1 ± 0.4 ms
BrIC	0.19 ± 0.06	0.22 ± 0.06	0.08 ± 0.03	0.1 ± 0.02	0.24 ± 0.08	0.22 ± 0.04
Medium Velocity						
PLA	118 ± 10 g	84 ± 17 g	101 ± 16 g	88 ± 2 g	105 ± 37 g	83 ± 8 g
PAV	16 ± 4 rad/s	14 ± 4 rad/s	6 ± 3 rad/s	6 ± 3 rad/s	21 ± 3 rad/s	20 ± 3 rad/s
PAA	5135 ± 827 rad/s/s	2223 ± 1031 rad/s/s	1116 ± 501 rad/s/s	1629 ± 439 rad/s/s	5618 ± 1847 rad/s/s	3978 ± 1840 rad/s/s
HIC	440 ± 103	175 ± 122	427 ± 149	289 ± 16	276 ± 165	187 ± 57
HIC Duration	5.4 ± 0.1 ms	11.2 ± 6.1 ms	7.0 ± 0.3 ms	7.9 ± 1.2 ms	4.6 ± 1.2 ms	7.8 ± 4.5 ms
BrIC	0.3 ± 0.08	0.31 ± 0.1	0.11 ± 0.05	0.18 ± 0.02	0.41 ± 0.07	0.36 ± 0.06
High Velocity						
PLA	205 ± 21 g	100 ± 10 g	140 ± 17 g	111 ± 5 g	200 ± 51 g	88 ± 2 g
PAV	17 ± 2 rad/s	13 ± 3 rad/s	9 ± 2 rad/s	9 ± 2 rad/s	30 ± 4 rad/s	25 ± 2 rad/s
PAA	5960 ± 1285 rad/s/s	1780 ± 521 rad/s/s	1710 ± 308 rad/s/s	1935 ± 849 rad/s/s	11133 ± 3150 rad/s/s	2887 ± 1106 rad/s/s
HIC	1119 ± 250	226 ± 96	774 ± 264	477 ± 68	850 ± 445	178 ± 47
HIC Duration	4.1 ± 0.3 ms	11.1 ± 4.4 ms	5.9 ± 0.2 ms	7.7 ± 1.6 ms	2.6 ± 0.3 ms	12.5 ± 4.2 ms
BrIC	0.31 ± 0.03	0.3 ± 0.08	0.18 ± 0.02	0.26 ± 0.07	0.6 ± 0.06	0.42 ± 0.04

TABLE AII
DTS iMG AND REFERENCE IMPACT METRICS

	Front (n=6)		**Rear (n=6)**		**Side (n=6)**	
	Reference	iMG	Reference	iMG	Reference	iMG
Low Velocity						
PLA	63 ± 21 g	219 ± 48 g	67 ± 11 g	79 ± 30 g	49 ± 10 g	58 ± 7 g
PAV	8 ± 2 rad/s	26 ± 4 rad/s	4 ± 2 rad/s	22 ± 5 rad/s	12 ± 1 rad/s	20 ± 5 rad/s
PAA	2237 ± 387 rad/s/s	13740 ± 4969 rad/s/s	788 ± 305 rad/s/s	4631 ± 3715 rad/s/s	2512 ± 172 rad/s/s	3420 ± 321 rad/s/s
HIC	130 ± 83	833 ± 639	166 ± 71	276 ± 301	64 ± 41	110 ± 15
HIC Duration	6.2 ± 0.6 ms	8.0 ± 1.4 ms	7.3 ± 0.3 ms	7.2 ± 1.1 ms	5.9 ± 1.3 ms	7.5 ± 0.8 ms
BrIC	0.16 ± 0.04	0.59 ± 0.12	0.08 ± 0.04	0.47 ± 0.15	0.24 ± 0.06	0.33 ± 0.06
Medium Velocity						
PLA	122 ± 27 g	243 ± 38 g	101 ± 22 g	113 ± 38 g	101 ± 42 g	137 ± 20 g
PAV	13 ± 4 rad/s	41 ± 11 rad/s	7 ± 3 rad/s	29 ± 3 rad/s	23 ± 1 rad/s	34 ± 2 rad/s
PAA	3774 ± 811 rad/s/s	13778 ± 4486 rad/s/s	1395 ± 371 rad/s/s	6256 ± 2924 rad/s/s	6449 ± 1534 rad/s/s	9649 ± 2456 rad/s/s
HIC	457 ± 206	1249 ± 818	440 ± 214	447 ± 219	265 ± 177	491 ± 58
HIC Duration	5.0 ± 1.1 ms	5.7 ± 1.3 ms	7.0 ± 0.4 ms	7.3 ± 1.0 ms	4.5 ± 1.1 ms	4.2 ± 1.2 ms
BrIC	0.25 ± 0.07	0.87 ± 0.13	0.12 ± 0.06	0.6 ± 0.12	0.46 ± 0.07	0.62 ± 0.04
High Velocity						
PLA	217 ± 14 g	348 ± 111 g	146 ± 25 g	165 ± 58 g	188 ± 83 g	254 ± 20 g
PAV	20 ± 5 rad/s	53 ± 37 rad/s	8 ± 3 rad/s	32 ± 4 rad/s	32 ± 4 rad/s	50 ± 5 rad/s
PAA	6061 ± 867 rad/s/s	17431 ± 6002 rad/s/s	1803 ± 492 rad/s/s	9603 ± 6433 rad/s/s	11822 ± 3427 rad/s/s	19376 ± 4780 rad/s/s
HIC	1276 ± 178	2651 ± 1743	782 ± 327	835 ± 437	819 ± 600	2392 ± 924
HIC Duration	4.7 ± 0.6 ms	7.3 ± 3.3 ms	5.4 ± 0.1 ms	5.6 ± 0.3 ms	3.0 ± 0.9 ms	7.1 ± 4.9 ms
BrIC	0.37 ± 0.08	1.14 ± 0.67	0.15 ± 0.06	0.64 ± 0.12	0.64 ± 0.05	0.96 ± 0.18

ERRATUM

Biofidelity and Limitations of Instrumented Mouthguard Systems for Assessment of Rigid Body Head Kinematics

Mitchell Z. Abrams, Jay Venkatraman, Donald Sherman, Maria Ortiz-Paparoni, Jefferson R. Bercaw, Robert E. MacDonald, Jason Kait, Elizabeth Dimbath, Derek Pang, Alexandra Gray, Jason F. Luck, Cynthia A. Bir, Cameron R. Bass

Following publication of the manuscript, the authors were alerted to two items in the introduction that require clarification, identified and amended below.

Where the original manuscript reads:
The iMG developed by Diversified Technical Systems (DTS) (Diversified Technical Systems, Seal Beach, CA, USA) was part of an effort with the National Football League (NFL) to measure head kinematics.

We here clarify the statement as:
The hardware within the DTS iMG, which collects and stores linear and angular acceleration, was part of an effort with Football Research, Inc to measure head kinematics for the NFL and NCAA.

Where the original manuscript reads:
Similarly, validation studies of the DTS iMG have found nearly one-to-one accuracy during ATD testing in both helmeted and unhelmeted test scenarios [20][23]

We here clarify the statement as:
Similarly, validation studies using mouthguards containing the DTS iMG hardware have found nearly one-to-one accuracy during ATD testing in both helmeted and unhelmeted test scenarios [20][23]